

Phase Stability in the Two dimensional Anisotropic Boson Hubbard Hamiltonian

T. Ying^{1,2}, G.G. Batrouni^{3,4,5}, V.G. Rousseau⁶, M. Jarrell⁶, J. Moreno⁶, X.D. Sun¹, and R.T. Scalettar²

¹*Department of Physics, Harbin Institute of Technology, Harbin 150001, China*

²*Physics Department, University of California, Davis, California 95616, USA*

³*INLN, Université de Nice–Sophia Antipolis, CNRS; 1361 route des Lucioles, 06560 Valbonne, France*

⁴*Institut Universitaire de France*

⁵*Centre for Quantum Technologies, National University of Singapore; 2 Science Drive 3 Singapore 117542 and*

⁶*Department of Physics and Astronomy, Louisiana State University, Baton Rouge, Louisiana 70803, USA*

The two dimensional square lattice hard-core boson Hubbard model with near neighbor interactions has a ‘checkerboard’ charge density wave insulating phase at half-filling and sufficiently large intersite repulsion. When doped, rather than forming a supersolid phase in which long range charge density wave correlations coexist with a condensation of superfluid defects, the system instead phase separates. However, it is known that there are other lattice geometries and interaction patterns for which such coexistence takes place. In this paper we explore the possibility that anisotropic hopping or anisotropic near neighbor repulsion might similarly stabilize the square lattice supersolid. By considering the charge density wave structure factor and superfluid density for different ratios of interaction strength and hybridization in the \hat{x} and \hat{y} directions, we conclude that phase separation still occurs.

PACS numbers: 71.10.Fd, 02.70.Uu

I. INTRODUCTION

In fermionic systems the competition between phase separation and (non-phonon mediated) superconductivity has been a long-standing and active area of research. On the one hand, Cooper pair formation requires an effective attractive interaction, but on the other hand this attraction might ‘go overboard’ and lead to the agglomeration of larger clusters of particles. This latter possibility is especially likely in commonly studied models of superconductivity like the Hubbard and t - J Hamiltonians^{1–7} which do not include a long-range Coulomb interaction that opposes phase separation.

A very similar set of issues arises in the interplay of Bose-Einstein condensation (and the closely related phenomenon of superfluidity) with charge order in bosonic systems, where the possibility of coexistence of diagonal and off-diagonal long range order is termed a ‘supersolid’ (SS) phase⁸. Bosonic systems are commonly studied in the continuum^{9,10}, motivated by liquid ⁴He. However, as with fermions, issues such as supersolidity can also be addressed within a tight-binding lattice model governed by the boson Hubbard Hamiltonian¹¹,

$$\begin{aligned} \hat{\mathcal{H}} = & - \sum_{ij} t_{ij} (a_i^\dagger a_j + a_j^\dagger a_i) + \frac{1}{2} \sum_i U_i n_i (n_i - 1) \\ & + \sum_{ij} V_{ij} n_i n_j - \sum_i \mu_i n_i \end{aligned} \quad (1)$$

Here a_i^\dagger , a_i , and n_i are boson creation, destruction, and number operators. t_{ij} is an intersite hopping between sites i and j . In this paper we consider a square lattice of linear size L and total number of sites $N = L^2$. U_i is an on-site repulsion, and V_{ij} is an intersite repulsion. The chemical potential μ controls the filling of the lattice.

Most studies of the boson-Hubbard Hamiltonian have considered the case of translationally invariant and short range interactions $U_i = U$, $V_{ij} = V_1(V_2)$ for near neighbor (next near neighbor) pairs ij , and near neighbor hopping $t_{ij} = t$. More complex choices for the Hamiltonian parameters are increasingly being studied, most notably situations in which the chemical potential models a quadratic trap to confine the bosons^{12–15}.

In the uniform interaction, hard-core limit, $U = \infty$, a site can be either empty or singly occupied. When a near neighbor, V_1 , is turned on at half-filling, the bosons begin to occupy only one of the two sublattices into which the square lattice is divided, owing to its bipartite character. For V_1 sufficiently large and at low temperature, this tendency becomes sufficiently pronounced to result in long range order: the boson occupations alternate in a checkerboard pattern, with a charge ordering vector $q = (\pi, \pi)$ and charge correlations extend to large separation. Doping away from half-filling creates defects in this charge density wave (CDW) phase. If the defect concentration is sufficiently low, it is possible that long range charge order is not destroyed, even though the defects can move through the ordered lattice and form a superfluid. In this way a supersolid would be realized.

However, it was shown^{16,17} that this coexistence does not occur for hardcore bosons on the 2D square lattice with near neighbor interactions. Rather, there is a thermodynamic instability to phase separation in which different spatial regions are superfluid and charge ordered. Despite the absence of simultaneous diagonal and off-diagonal long range order in this most simple scenario, other lattice geometries have been shown to exhibit supersolid phases, and, indeed, by now there is a considerable numerical literature as a function of lattice geometry, dimensionality, filling and interaction^{18–37}. More exotic processes within the Hamiltonian, such as

ring exchange, are also known to play a potential role in supersolidity^{38,39}.

One of the lines of investigation into supersolidity has pursued the effect of anisotropy. Thus, although the checkerboard supersolid with $q = (\pi, \pi)$ ordering wavevector is unstable, it was also shown that a striped supersolid is stable¹⁷. Such a phase is caused by a next-near neighbor interaction V_2 which drives charge order at wavevector $q = (\pi, 0)$ or $(0, \pi)$ which is then doped to allow for mobile defects. In this case the underlying Hamiltonian is isotropic, but a spontaneous breaking of the Z_2 symmetry associated with order along the \hat{x} or \hat{y} directions occurs. Recent studies have also shown that symmetry breaking in the Hamiltonian itself can give rise to striped supersolids. In particular, Chan *et al.*⁴⁰ argued that an attractive interaction in one spatial direction and a repulsive interaction in the other will cause supersolid formation.

These known instances of stability of the striped supersolid, as well as the general delicacy of the energy balance involved in whether phase separation occurs or not⁶, suggest that a checkerboard supersolid might be stabilized by anisotropic hoppings $t_x \neq t_y$ or interactions $V_x \neq V_y$ in the \hat{x} and \hat{y} directions. This is the topic of the present paper. Stable supersolid phases have already been found for soft-core bosons in one, two and three dimensions^{22,23,36,37,41}. When the contact repulsion, U , is large compared to the near neighbor interaction, V_1 , (the mean field value is $U > 4V_1$ in two dimensions), the system behaves as in the hard core case and phase separates when doped away from half filling. When V_1 dominates, $U < 4V_1$, and the system is doped above half filling, the extra bosons will go on already occupied sites. These doubly occupied defects then delocalize and yield a supersolid phase. On the other hand, if the system is doped below half-filling, it will typically undergo phase separation. Remarkably, however, there is a very narrow parameter range where the system will become supersolid when doped below half filling^{36,37}. This history of successful searches for supersolidity in soft-core models prompts us to focus here on the hard-core case.

After introducing our Quantum Monte Carlo methodology and the observables used to characterize the phases, we show results indicating that supersolids do not emerge from a checkerboard charge ordered pattern driven by near-neighbor interactions, even when those interactions or the hoppings are made anisotropic. The dependences of the superfluid density ρ_s and the CDW structure factor $S(q)$ on V_{1x}/V_{1y} and t_x/t_y are calculated.

II. METHODOLOGY

Our computational approach is the stochastic Green function (SGF) approach^{42–44}. SGF is a finite temperature Quantum Monte Carlo algorithm which

works in continuous imaginary time (avoiding the need to extrapolate to zero discretization mesh of the inverse temperature β). Here we use a recent new formulation of the method which includes global space-time updates⁴⁵ to explore phase space efficiently and to sample the winding and hence superfluid density. We use a canonical formulation which allows us to work with fixed particle number, although the method can also be implemented in the grand canonical ensemble. Note that even within a canonical implementation, it is still possible to obtain the chemical potential as a finite difference of ground state energies at adjacent particle numbers, $\mu(n) = E_0(n+1) - E_0(n)$.

We will characterize the phases of the Hamiltonian Eq. 1 by examining the energy, $E = \langle H \rangle$ and also the superfluid density ρ_s and CDW structure factor $S(q)$. The superfluid density is obtained using the procedure described by Pollock and Ceperley⁹, in which ρ_s is expressed in terms of the winding W of bosonic world lines across a lattice edge.

$$\rho_{sx} = \frac{\langle W_x^2 \rangle}{2\beta t_x} \quad \rho_{sy} = \frac{\langle W_y^2 \rangle}{2\beta t_y} \quad (2)$$

Here we have allowed for the possibility of inequivalent spatial directions, and measure the x and y superfluid densities separately.

The CDW structure factor is the Fourier transform of the density-density correlation function.

$$S(q) = \frac{1}{N^2} \sum_{jl} e^{iq \cdot l} \langle n_j n_{j+l} \rangle \quad (3)$$

Here N is the number of sites. In order to establish long range order, both ρ_s and $S(q)$ must be extrapolated to the $N \rightarrow \infty$ limit via finite size scaling.

The choice of how to compare anisotropic lattices with isotropic ones is somewhat arbitrary. Here we have chosen to keep $t_x + t_y$ fixed as we vary t_x away from t_y , rather than, for example, fixing t_y and reducing t_x to zero. Our rationale is that this preserves the overall noninteracting bandwidth $W = 4(t_x + t_y)$. Similarly, when we vary the interactions we do so by fixing the sum $V_{1x} + V_{1y}$. The motivation behind this choice is that in the strong coupling limit the energy cost to add a particle to a perfect checkerboard solid, $2(V_{1x} + V_{1y})$ is preserved. That is, the “base of the insulating lobes”¹¹ at $t = 0$ is the same for all degrees of anisotropy.

III. RESULTS

A. Interaction Anisotropy

We begin by considering $t_x = t_y$ but $V_{1x} \neq V_{1y}$. Figure 1 shows the checkerboard structure factor $S(\pi, \pi)$ and superfluid density ρ_s as functions of filling ρ . In Figure 1(a), $S(\pi, \pi)$ is robust to anisotropy, declining

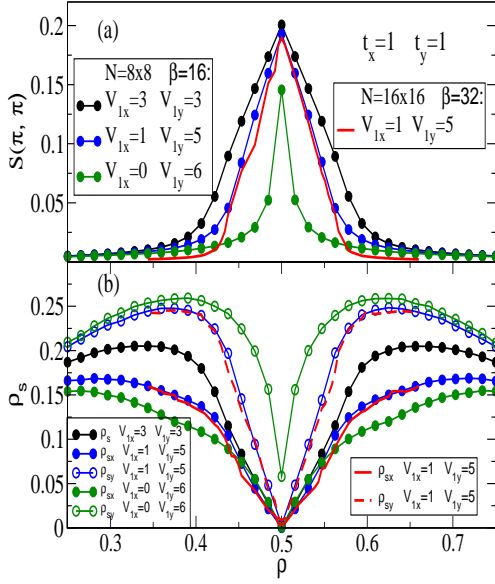


FIG. 1: (Color online) Checkerboard structure factor (a) and superfluid density (b) as functions of filling, comparing anisotropic near neighbor interaction strengths V_{1x}, V_{1y} with isotropic ones. $S(\pi, \pi)$ is relatively unaffected by shifting V_{1x} away from V_{1y} : the data for $V_{1x} = 1, V_{1y} = 5$ declines somewhat more rapidly with doping away from $\rho = 1$ but looks qualitatively quite similar. Only when $V_{1x} = 0$ does the structure factor change behavior significantly. Similar remarks apply to the superfluid density. Superflow ρ_{sy} in the \hat{y} direction is larger than that in the \hat{x} direction. Most data are for 8×8 lattices at $\beta = 16$, but lines without symbols are for 16×16 lattices at $\beta = 32$ and show that finite spatial lattice and temperature effects are minimal. Here and in subsequent figures error bars are smaller than the symbol size and hence are not shown.

only modestly from its value at $V_{1x} = 3, V_{1y} = 3$ to its value at $V_{1x} = 1, V_{1y} = 5$. However, when $V_{1x} = 0$, $S(\pi, \pi)$ is greatly altered. In this limit, if the hopping t is neglected, the lattice decomposes into independent chains each with density order at $q_y = \pi$ but arbitrary q_x . Figure 1 indicates that nonzero V_{1x} locks these chains into place spatially (selecting out $q_x = \pi$ as well). This is likely due to the enhanced kinetic energy when hard core bosons in one chain find empty sites on neighboring chains. This robustness of checkerboard order in the $V_{1x} = 0$ limit is confined to $\rho = 0.5$. The structure factor falls off much more abruptly with doping than when V_{1x} remains nonzero.

The behavior of ρ_s in Figure 1(b) is also largely unaffected by anisotropy. The largest change is an enhancement of ρ_s in the vicinity of the insulating solid phase at half-filling. Surprisingly, the details of the choice of interaction strength become unimportant at low density (and high density due to particle-hole symmetry). The x and y components of the superfluid response, ρ_{sx} and ρ_{sy} , have the same qualitative dependence on density ρ , although for the largest anisotropy $V_{1x} = 0$, ρ_{sy} is

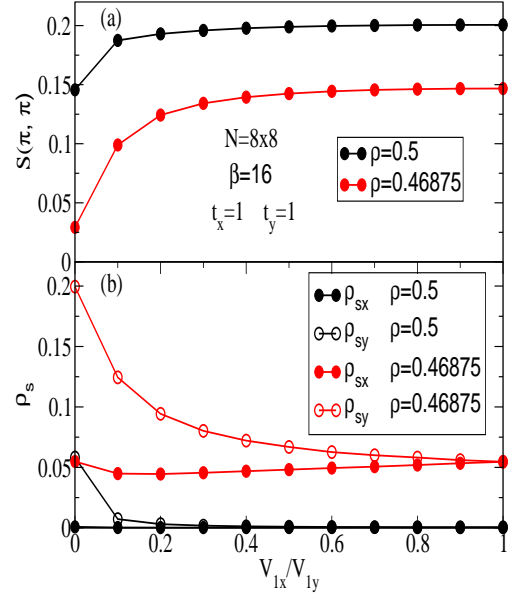


FIG. 2: (Color online) (a) $S(\pi, \pi)$ vs V_{1x}/V_{1y} at half-filling $\rho = 0.5$ and lightly doped $\rho = 15/32$. The sum $V_{1x} + V_{1y} = 6$ is fixed. The flatness of the data except in the vicinity of $V_{1x}/V_{1y} = 0$ emphasizes the minor effects of anisotropic interactions, especially at half-filling. (b) ρ_{sx} and ρ_{sy} vs V_{1x}/V_{1y} at the same two densities. The system is insulating for $\rho = 0.5$ except strictly in the $V_{1x} = 0$ limit. In the doped case, ρ_{sx} shows little change with anisotropy, while ρ_{sy} increases sharply near $V_{1x} = 0$. Spatial lattice size is 8×8 and inverse temperature $\beta = 16$.

roughly twice ρ_{sx} for all densities. A precise picture of the interplay of the anisotropies in charge correlations and superfluidity is not clear. Since $V_{1x} \ll V_{1y}$ it is more likely that \hat{x} neighbors will both be occupied (or empty) than \hat{y} neighbors. Strings of adjacent occupied sites of hard-core bosons would seemingly block motion perpendicular to them (and hence suppress ρ_{sy}). Meanwhile, strings of adjacent empty sites would offer channels for an enhanced ρ_{sy} . A complicating feature of any attempt to build such a ‘blocking/channel’ picture is the fact that while the hard-core nature of the bosons completely precludes certain types of motion, the strong V_{1y} interactions will also profoundly affect the pattern of bosonic flow. The small non-zero value of ρ_{sy} at $V_{1x} = 0$ and half-filling is a finite lattice effect. (See Fig. 4.)

The detailed evolution of the CDW structure factor and superfluid densities with interaction anisotropy V_{1x}/V_{1y} is given in Fig. 2. Panel (a) emphasizes that $S(\pi, \pi)$ is generally robust to anisotropy at half-filling $\rho = 0.5$, but can change dramatically for sufficiently small V_{1x}/V_{1y} when the system is (slightly) doped to $\rho = 15/32$. Panel (b) indicates similarly that ρ_s is much more affected by anisotropy in the presence of vacancies. Bosons flow more freely in the direction perpendicular to that for which the repulsive interaction is smaller. This probably represents the low energy cost of lines of bosons

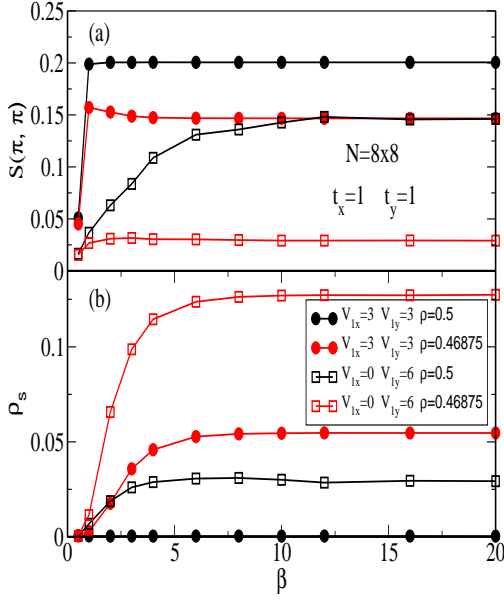


FIG. 3: (Color online) The temperature dependence of (a) structure factor $S(\pi, \pi)$ and (b) superfluid density ρ_s (averaged over the \hat{x} and \hat{y} directions) are shown. We see that for $\beta \geq 10$, these quantities take their ground state values for the parameters we are using.

which have strong charge ordering in the \hat{y} direction slipping past each other due to the minimal energy cost in V_{1x} . Of course such a picture is a bit naive in the present case when the system undergoes phase separation and consists of a mixture of superfluid and CDW regions.

Figure 1(a,b) contained some comparison of data on different lattice sizes. Fig. 3 and Fig. 4 show the effects of temperature $T = 1/\beta$ and L more systematically. Fig. 3 establishes that the system is in the ground state when $\beta \approx 10$, validating the choice of $\beta = 16$ used to access the ground state in Fig. 1. The approach to the low temperature limit is somewhat more gradual in the extreme anisotropic case $V_{1x} = 0$. Fig. 4 allows an extrapolation to the thermodynamic limit $1/L \rightarrow 0$. As at half-filling, for a doping $\rho = 15/32$ the CDW structure factor $S(\pi, \pi)$ is nonzero at large L . Further doping to $\rho = 13/32$ destroys long range density order. The anisotropic system is more sensitive to doping than when $V_{1x} = V_{1y}$.

Figures 1, 3, 4 establish the possibility of a supersolid phase: Non-zero ρ_s coexists with large $S(\pi, \pi)$ in the vicinity of half-filling. However, it is necessary to distinguish a true supersolid phase, in which these orders coexist as a single stable thermodynamic phase, from a lattice in which both orders are present at separate spatial locations. This phase separation is most easily detected by looking for an anomalous negative curvature, $d^2E/d\rho^2 < 0$, in the thermodynamics. Figure 5 shows that such negative curvature is present just below $\rho = 0.5$, unless $V_{1x} = 0$.

The jump in slope $\mu = dE/d\rho$ at $\rho = 0.5$ is the charge

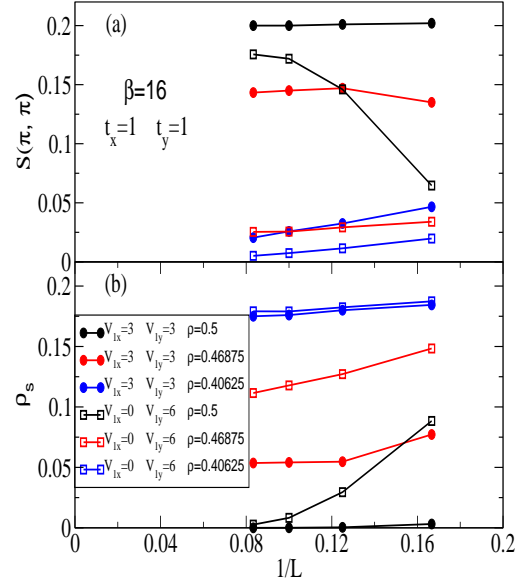


FIG. 4: (Color online) The lattice size dependences of (a) structure factor $S(\pi, \pi)$ and (b) superfluid density ρ_s are shown. Solid circles are the isotropic case $V_{1x} = V_{1y} = 3$. The system retains checkerboard CDW order when the doping is small ($\rho = 15/32$) but not for $\rho = 13/32$. Open squares are the extreme anisotropic case $V_{1x} = 0$. In that case there is order only at half-filling. ρ_s is larger when the interactions are anisotropic, but the finite size scaling indicates that it still vanishes at half-filling in the thermodynamic limit even when $V_{1x} = 0$.

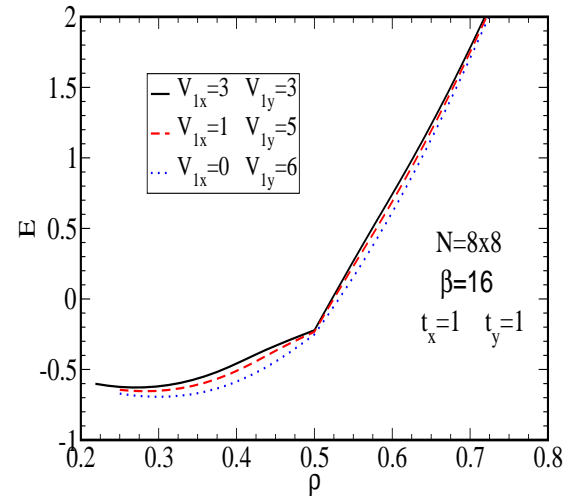


FIG. 5: (Color online) Energy E as a function of density ρ exhibits the characteristic signal of phase separation $d^2E/d\rho^2 < 0$ as long as V_{1x} remains non-zero. The kinks at half-filling imply an abrupt jump in chemical potential, that is, the presence of a non-zero charge gap.

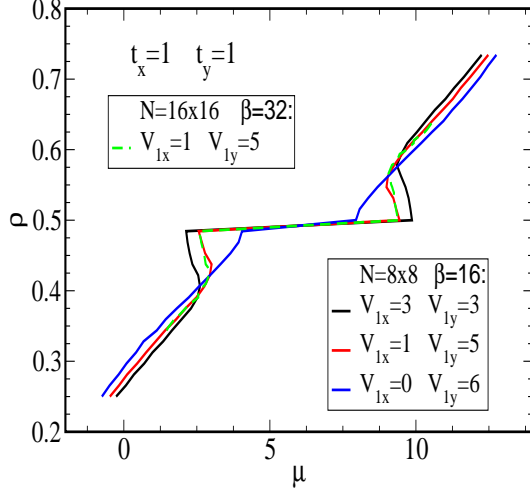


FIG. 6: (Color online) Phase separation is indicated by a chemical potential μ which decreases as ρ approaches $\rho = 0.5$ from below. This phenomenon, previously established in the isotropic case, is still present with anisotropy, except in the extreme limiting case $V_{1x} = 0$. Results for 8×8 lattices at $\beta = 16$ and 16×16 lattices at $\beta = 32$ show finite-size and finite temperature effects are negligible both for the size of the Mott gap and the negative curvature (phase separation).

gap Δ_c . Figure 6 shows the density ρ as a function of chemical potential μ . The kink at half-filling in Fig. 5 is reflected in a plateau in the density. As commented earlier, fixing $V_{1x} + V_{1y}$ makes the length of this plateau $\Delta_c = 2(V_{1x} + V_{1y})$ the same for all degrees of anisotropy in the strong coupling ($t \rightarrow 0$) limit. Figure 6 indicates that finite hopping $t = 1$ reduces Δ_c from the $t = 0$ value $\Delta_c = 12$ to $\Delta_c \sim 8$. There is only a relatively small reduction in Δ_c going from $V_{1x} = V_{1y} = 3$ to $V_{1x} = 1, V_{1y} = 5$. Setting $V_{1x} = 0$, however, reduces the gap to $\Delta_c \sim 4$.

In Fig. 6 the signature of phase separation is made more evident, in the form of a double valued dependence of density on chemical potential $\mu = dE/d\rho$. In other words, the chemical potential μ is not a monotonically increasing function of density ρ . The usual Maxwell construction can be used to ascertain the relative sizes of the superfluid and solid regions in this situation. The instability of the checkerboard supersolid in the isotropic case is known¹⁷. Figures 5 and 6 establish that this instability persists in the anisotropic case, except in the extreme case of vanishing interchain interaction, $V_{1x} = 0$. However, as seen in Fig. 1, the structure factor falls off rapidly with doping in this situation, so that long range density (solid) order is no longer present. Thus the absence of phase separation does not imply the existence of a supersolid.

Figure 7 shows the individual components of the

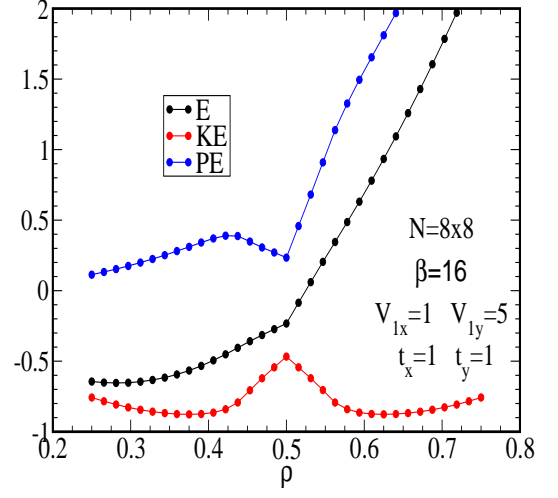


FIG. 7: (Color online) Kinetic, potential, and total energies as functions of the filling ρ . The kinetic energy is minimized (in absolute value) at half-filling, as expected for an insulating solid. Phase separation appears to be driven primarily by the density dependence of the potential energy, whose decrease from a maximum at $\rho \approx 0.43$ results in the negative curvature in the total energy.

energy. At $\rho = 0.5$ the system is in an insulating checkerboard solid phase, and has a corresponding minimum in the absolute value of the kinetic energy. The potential energy at first increases from the low density limit, reflecting the increased likelihood of adjacently occupied sites. At $\rho \approx 0.43$, however, the potential energy decreases, despite a rising number of particles. Presumably this reflects the onset of density order: a coherent pattern of occupation in which adjacent sites are rarely occupied. Evidently, the decrease of $\langle n_i n_j \rangle$ for near neighbor sites ij associated with solid formation overwhelms the ‘trivial’ increase $\langle n_i n_j \rangle \propto \langle n_i \rangle \langle n_j \rangle$ expected for noninteracting bosons.

B. Hopping Anisotropy

Having explored the possibility of supersolids caused by anisotropy in the near neighbor interaction we turn to the analogous question when $t_x \neq t_y$. Figure 8 shows the checkerboard structure factor $S(\pi, \pi)$ and superfluid densities ρ_{sx} and ρ_{sy} in the \hat{x} and \hat{y} directions. The structure factor is peaked at half-filling but remains relatively large in some interval surrounding that density. In general $\rho_{sx} > \rho_{sy}$, the superflow in the \hat{x} direction shows a dip at fillings $\rho = 3/8$ and $\rho = 5/8$. This dip becomes more pronounced as the hopping anisotropy increases. We will address this issue, which requires some challenging QMC simulations and which is not directly

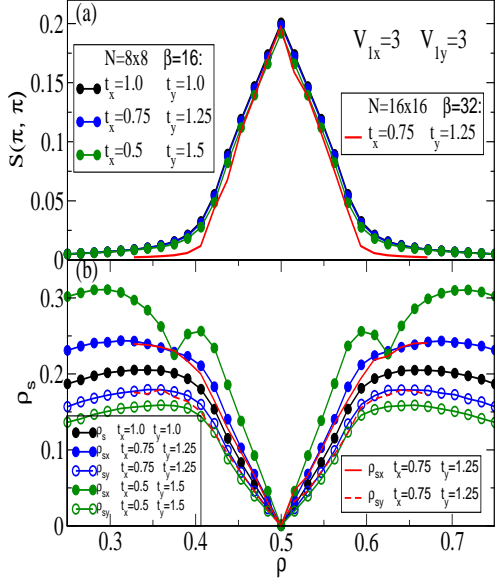


FIG. 8: (Color online) Checkerboard structure factor $S(\pi, \pi)$ (top), along with superfluid densities ρ_{sx} and ρ_{sy} in the \hat{x} and \hat{y} directions (bottom). $S(\pi, \pi)$ is large in the vicinity of half-filling and decreases with doping. It is almost unchanged by hopping anisotropy. The superfluid density vanishes at half-filling, and rises with doping. Beginning with $\rho_{sx} = \rho_{sy}$ for $t_x = t_y$, the superfluid density in the \hat{x} direction shifts upward, and that in the \hat{y} direction downward, as t_x/t_y decreases. Results for 16x16 lattices at $\beta = 32$ show that finite spatial lattice and temperature effects are minimal. For the largest hopping anisotropy, ρ_{sx} has a dip at fillings $\rho = 3/8, 5/8$. This will be discussed in a subsequent work.

related to the questions being addressed here⁴⁶, in a later paper.

The thermodynamics, shown in $E(\rho)$ (Fig. 9) and $\rho(\mu)$ (Fig. 10) show some features similar to those seen in the anisotropic interaction case. $E(\rho)$ exhibits a kink at $\rho = 0.5$ indicating a jump in the chemical potential and hence a charge gap, and also negative curvature (phase separation) in the vicinity of half-filling. $\rho(\mu)$ demonstrates these features even more directly. The gap (plateau in $\rho(\mu)$) is unchanged even for a case when the ratio of hoppings is altered by a factor of three from $t_x/t_y = 1$ to $t_x/t_y = 1/3$. This is in contrast to interaction anisotropy to which the gap is more sensitive (Figure 6).

Figure 11 provides quantitative detail on the evolution of the CDW structure factor and superfluid densities with hopping anisotropy. For both densities, the data for $S(\pi, \pi)$ are quite flat over the range shown, $1/3 < t_x/t_y < 1$. The superfluid densities, especially in the \hat{x} direction show significant quantitative evolution⁴⁸, but qualitatively they are unchanged, indicating superfluid behavior for density $\rho = 15/32$ and insulating behavior for half-filling $\rho = 1/2$.

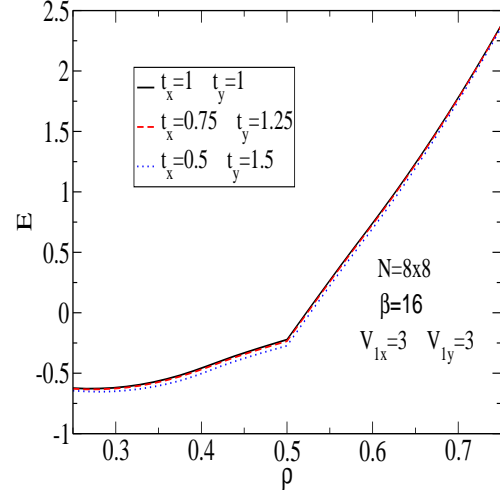


FIG. 9: (Color online) Energy $E(\rho)$ for three different hopping anisotropies. All have the kink which signals the Mott gap, and also negative curvature (phase separation) in the vicinity of half-filling.

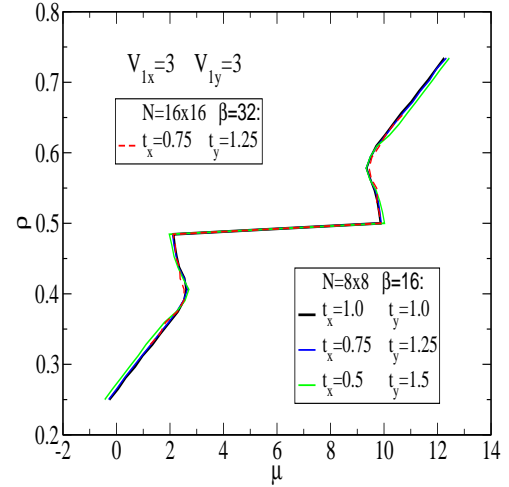


FIG. 10: (Color online) Dependence of filling on chemical potential $\rho(\mu)$, extracted from energy data of Fig. 9. At half-filling, a plateau in $\rho(\mu)$ signals the charge-ordered insulator, with adjacent densities showing a thermodynamic instability to phase separation. Data for 16x16 lattices at $\beta = 32$ show that finite spatial lattice and temperature effects are minimal both for the size of the Mott gap and the negative curvature. The charge gap and negative curvature are largely independent of the degree of hopping anisotropy, even though $t_{1y}/t_{1x} = 3$ is fairly large. Some of this invariance is due to our choice $t_{1x} + t_{1y} = 2$, which keeps the noninteracting bandwidth fixed.

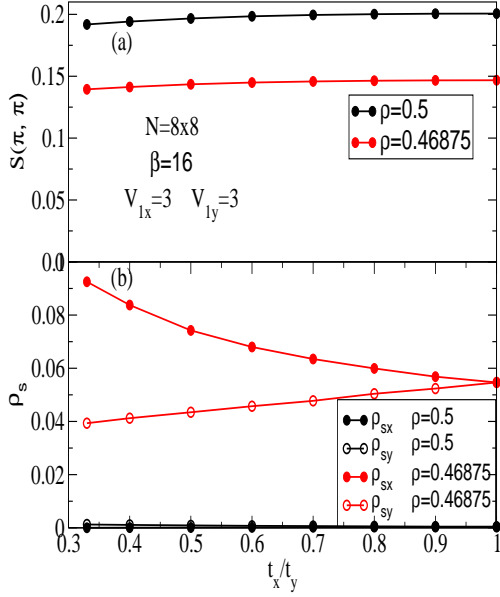


FIG. 11: (Color online) (a): $S(\pi, \pi)$ vs t_x/t_y at $\rho = 0.5$ and $\rho = 15/32$. The structure factor is even less sensitive to hopping anisotropy than to interaction anisotropy, as might perhaps be expected since charge order is directly driven by V as opposed to t . (b): ρ_{sx} and ρ_{sy} vs t_x/t_y at $\rho = 0.5$ and $\rho = 15/32$. The sum $t_x + t_y = 2$ for all data here.

IV. CONCLUSIONS

The simultaneous presence of diagonal and off-diagonal long range order, as opposed to a transition between distinct ordered phases, is by now well-established in many bosonic models. In this paper we have shown

that this coexistence is thermodynamically unstable in a broad range of square lattice hard-core Hamiltonians with near neighbor interactions and hopping parameters which break x - y symmetry. Although our results are for choices in which only hopping or interactions are anisotropic, we have also studied a few cases where x / y symmetry is broken in both terms⁴⁹. These more complex situations also exhibited phase separation as opposed to supersolidity. Of course, we cannot exclude the possibility that a supersolid is stable in some other choice of parameter values.

The motivation for studying such situations is to gain a more complete understanding of the interplay between real space particle arrangements and superflow in quantum systems. For strongly correlated fermions, this is a central puzzle of unconventional superconductivity: Do antiferromagnetic (AF) and charge order (stripes) compete or coexist with pairing? These issues arise not only in cuprate materials, which have AF ordering at $q = (\pi, \pi)$ but also in the more recently discovered iron-pnictides whose magnetic ordering is at $q = (0, \pi)$: AF in one direction and ferromagnetic in the other.

Since bosonic systems are more simple to study computationally than fermionic ones, it would be interesting to extend the present work to ‘spin-1/2’ bosons⁴⁷ where one might have the analogs of both spin and charge order along with the possibility of superfluidity.

This work was supported by: the National Key Basic Research Program of China Grant No. 2013CB328702; a CNRS-UC Davis EPOCAL LIA joint research grant; by NSF-PIF-1005503; DOE SSAAP de-na0001842-0; DOE SciDAC Grant No. DE-FC02-06ER25792 and NSF OISE-0952300. We thank B. Brummels for useful input.

- ¹ V.J. Emery, S.A. Kivelson, and H.Q. Lin, Phys. Rev. Lett. **64**, 475 (1990).
- ² M. Marder, N. Papanicolaou, and G.C. Psaltakis, Phys. Rev. B **41**, 6920 (1990)
- ³ C. Stephen Hellberg and E. Manousakis, Phys. Rev. Lett. **78**, 4609 (1997).
- ⁴ J.A. Riera and A.P. Young, Phys. Rev. B **39**, 9697 (1989).
- ⁵ E. Dagotto, A. Moreo, R.L. Sugar, and D. Toussaint, Phys. Rev. B **41**, 811 (1990).
- ⁶ R.M. Fye, M.J. Martins, and R.T. Scalettar, Phys. Rev. B **42**, 6809 (1990).
- ⁷ C.-C. Chang and S. Zhang, Phys. Rev. B **78**, 165101 (2008).
- ⁸ O. Penrose, and L. Onsager, Phys. Rev. **104**, 576 (1956). A. F. Andreev, and I. M. Lifshitz, Sov. Phys. JETP **29**, 1107 (1960); G. Chester, Phys. Rev. A **2**, 256 (1970); A. J. Leggett, Phys. Rev. Lett. **25**, 1543 (1970).
- ⁹ E.L. Pollock and D.M. Ceperley, Phys. Rev. B **36**, 8343 (1987).
- ¹⁰ S.A. Khairallah and D.M. Ceperley, Phys. Rev. Lett. **95**, 185301 (2005).
- ¹¹ M.P.A. Fisher, P.B. Weichman, G. Grinstein, and D.S. Fisher Phys. Rev. B **40**, 546 (1989).
- ¹² V.A. Kashurnikov, N.V. Prokofev, and B.V. Svistunov, Phys. Rev. A **66**, 031601 (2002).
- ¹³ G.G. Batrouni, V. Rousseau, R.T. Scalettar, M. Rigol, A. Muramatsu, P.J.H. Denteneer, and M. Troyer, Phys. Rev. Lett. **89**, 117203 (2002).
- ¹⁴ S. Wessel, F. Alet, M. Troyer, and G.G. Batrouni, Phys. Rev. A **70**, 053615 (2004).
- ¹⁵ G.G. Batrouni, H.R. Krishnamurthy, K.W. Mahmud, V.G. Rousseau, and R.T. Scalettar, Phys. Rev. A **78** 023627 (2008).
- ¹⁶ G.G. Batrouni, R.T. Scalettar, G.T. Zimanyi, and A.P. Kampf, Phys. Rev. Lett. **74** 2527 (1995).
- ¹⁷ G.G. Batrouni and R.T. Scalettar, Phys. Rev. Lett. **84**, 1599 (2000).
- ¹⁸ A. van Otterlo, K. H. Wagenblast, R. Baltin, C. Bruder, R. Fazio, and G. Schön, Phys. Rev. B **52**, 16176 (1995).
- ¹⁹ K. Góral, L. Santos, and M. Lewenstein, Phys. Rev. Lett. **88**, 170406 (2002).
- ²⁰ S. Wessel and M. Troyer, Phys. Rev. Lett. **95**, 127205 (2005).
- ²¹ M. Boninsegni and N. Prokofev, Phys. Rev. Lett. **95**,

- 237204 (2005).
- ²² P. Sengupta, L. P. Pryadko, F. Alet, M. Troyer, and G. Schmid, Phys. Rev. Lett. **94**, 207202 (2005).
 - ²³ G.G. Batrouni, F. Hébert, and R.T. Scalettar, Phys. Rev. Lett. **97**, 087209 (2006).
 - ²⁴ V.W. Scarola, E. Demler, and S. Das Sarma, Phys. Rev. **A 73**, 051601(R) (2006).
 - ²⁵ S. Yi, T. Li, and C. P. Sun, Phys. Rev. Lett. **98**, 260405 (2007).
 - ²⁶ T. Suzuki and N. Kawashima, Phys. Rev. **B 75**, 180502(R) (2007).
 - ²⁷ J-Y Gan, Y-C Wen, and Y. Yu Phys. Rev. **B 75**, 094501 (2007) .
 - ²⁸ L. Dang, M. Boninsegni, and L. Pollet, Phys. Rev. **B 78**, 132512 (2008).
 - ²⁹ K. Yamamoto, S. Todo, and S. Miyashita, Phys. Rev. **B 79**, 094503 (2009).
 - ³⁰ I. Danshita and C. A. R. Sá de Melo, Phys. Rev. Lett. **103**, 225301 (2009).
 - ³¹ L. Pollet, J. D. Picon, H. P. Büchler, and M. Troyer, Phys. Rev. Lett. **104**, 125302 (2010).
 - ³² B. Capogrosso-Sansone, C. Trefzger, M. Lewenstein, P. Zoller, and G. Pupillo, Phys. Rev. Lett. **104**, 125301 (2010).
 - ³³ B. Xi, F. Ye, W. Chen, F. Zhang, and G. Su, Phys. Rev. **B 84**, 054512 (2011).
 - ³⁴ D. Yamamoto, I. Danshita, and C.A.R. Sá de Melo, Phys. Rev. **A 85**, 021601(R) (2012).
 - ³⁵ H-C. Jiang, L. Fu, and C. Xu, Phys. Rev. **B 86**, 045129 (2012).
 - ³⁶ T. Ohgoe, T. Suzuki, and N. Kawashima, Phys. Rev. Lett. **108**, 185302 (2012).
 - ³⁷ T. Ohgoe, T. Suzuki, and N. Kawashima, Phys. Rev. **B 86**, 054520 (2012).
 - ³⁸ D.M. Ceperley and B. Bernu, Phys. Rev. Lett. **93**, 155303 (2004).
 - ³⁹ V.G. Rousseau, R.T. Scalettar, and G.G. Batrouni, Phys. Rev. **B 72**, 054524 (2005).
 - ⁴⁰ Y.-H. Chan, Y.-J. Han, and L.-M. Duan, Phys. Rev. **A 82**, 053607 (2010).
 - ⁴¹ G.G. Batrouni, R.T. Scalettar, V. G. Rousseau, B. Grémaud, arXiv:1304.2120.
 - ⁴² V.G. Rousseau, Phys. Rev. **E 77**, 056705 (2008).
 - ⁴³ V.G. Rousseau, Phys. Rev. **E 78**, 056707(2008).
 - ⁴⁴ Although this capability is not needed for the situation studied here, the SGF method is especially suited to complex models containing general four and six operator terms in the Hamiltonian.
 - ⁴⁵ V.G. Rousseau and D. Galanakis, arXiv:1209.0946.
 - ⁴⁶ F. Crepin, N. Laflorencie, G. Roux, and P. Simon, Phys. Rev. **B 84**, 054517 (2011).
 - ⁴⁷ L. de Forges de Parny, M. Traynard, F. Hébert, V.G. Rousseau, R.T. Scalettar, and G.G. Batrouni, Phys. Rev. **A 82**, 063602 (2010).
 - ⁴⁸ In principle, one might ask why the anisotropy breaks the symmetry between ρ_{sx} and ρ_{sy} in the way it does, i.e. why $\rho_{sx} > \rho_{sy}$ when $t_x < t_y$. However, it is unclear whether there is a meaningful answer to this question in this case where the system phase separates.
 - ⁴⁹ Specifically, we simulated (a) $t_x = 0.25, V_x = 1, t_y = 1.75, V_y = 5$; and (b) $t_x = 0.25, V_x = 5, t_y = 1.75, V_y = 1$.